

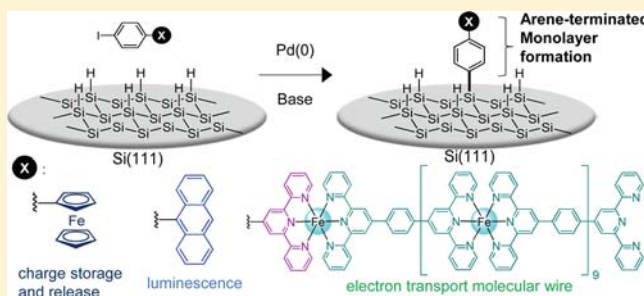
# A New Method To Generate Arene-Terminated Si(111) and Ge(111) Surfaces via a Palladium-Catalyzed Arylation Reaction

Yoshinori Yamanoi,\* Junya Sendo, Tetsuhiro Kobayashi, Hiroaki Maeda, Yusuke Yabusaki, Mariko Miyachi, Ryota Sakamoto, and Hiroshi Nishihara\*

Department of Chemistry, School of Science, The University of Tokyo, 7-3-1 Hongo, Bunkyo-ku, Tokyo 113-0033, Japan

**S** Supporting Information

**ABSTRACT:** Formation of silicon–aryl and germanium–aryl direct bonds on the semiconductor surface is a key issue to realize molecular electronic devices, but the conventional methods based on radical intermediates have problems to accompany the side reactions. We developed the first example of versatile and efficient methods to form clean organic monolayers with Si–aryl and Ge–aryl bonds on hydrogen-terminated silicon and germanium surfaces by applying our original catalytic arylation reactions of hydrosilanes and hydrogermanes using Pd catalyst and base in homogeneous systems. We could immobilize aromatic groups with redox-active and photoluminescent properties, and further applied in the field of rigid  $\pi$ -conjugated redox molecular wire composites, as confirmed by the successive coordination of terpyridine molecules with transition metal ions. The surfaces were characterized using cyclic voltammetry (CV), water contact angle measurements, X-ray photoelectron spectroscopy (XPS), fluorescence spectroscopy, and atomic force microscopy (AFM). Especially, the AFM analysis of 17 nm-long metal complex molecular wires confirmed their vertical connection to the plane surface.



## INTRODUCTION

In recent years, semiconductor surfaces terminated with organic compounds have attracted considerable interest, because of the scientific importance of heterointerfaces. The attachment of functional monolayers onto silicon surfaces is an attractive approach for the construction of novel interfaces for molecular electronics applications. The organic modification of hydrogen-terminated silicon surfaces with Si–C bonds provides electronic coupling between organic functionalities and semiconductors without the interference of interfacial oxide thin films.<sup>1–4</sup> Various modification methods have been investigated for the formation of Si–C bonded organic monolayers on silicon surfaces, including the hydrosilylation of alkenes or alkynes. The immobilization of aryl groups on oxide-free silicon is less common, although it is useful because the common aryl groups are chemically and thermally stable, structurally rigid, and electronically conductive, and thus suitable for controlling the geometric configuration and electronic interaction of the attached molecules with the semiconductor substrate. In the conventional methods, the Si–aryl bond formation is generally performed using aryl diazonium salts<sup>5–8</sup> or via the electrografting of iodonium salts.<sup>9</sup> However, not monolayer formation but multilayer formation is facilitated by the high reactive radical intermediates used in these methods. Establishing that there is a covalent bond between the aryl group monolayer and the electrode surface is a complex task.

In the course of our studies on the transition-metal-mediated transformation of hydrosilanes and hydrogermanes with aryl

halides (Figure 1a),<sup>10–17</sup> we recently reported the palladium-catalyzed arylation of the triply  $\sigma$ -back bonded silane, tris(trimethylsilyl)silane, in the presence of an organic base.<sup>18</sup> Arylated products were obtained in good to high yields, without breaking the weak Si–Si back bonds (Figure 1b). The surface modification was directed by the model reactions of aryl iodides and tris(trimethylsilyl)silane, which is a molecular model for the Si–H group on hydrogen-terminated silicon(111) surfaces (Si(111)–H). Because this transformation occurs under mild conditions and is compatible with a large number of terminal group functionalities, it is of interest to determine if this homogeneous catalytic process can be utilized to a heterogeneous reaction to produce a clean aromatic monolayer on silicon surfaces. Because of the attractive electrochemical properties of ferrocene-containing molecule (1), heteroaromatic molecule (2), photoluminescence properties of anthracene-containing molecule (3), and good metal-coordination abilities of terpyridine-containing molecule (4), we showed in this study that they can be effectively immobilized onto Si(111)–H and Ge(111)–H to form a monolayer (Figure 1c).

## MATERIAL AND METHODS

**Chemicals.** All synthetic procedures were carried out in an inert atmosphere. Compounds 1<sup>19</sup> and 4<sup>20</sup> were prepared according to known methods. Compound 3 was synthesized by Suzuki coupling.

Received: August 30, 2012

Published: November 26, 2012

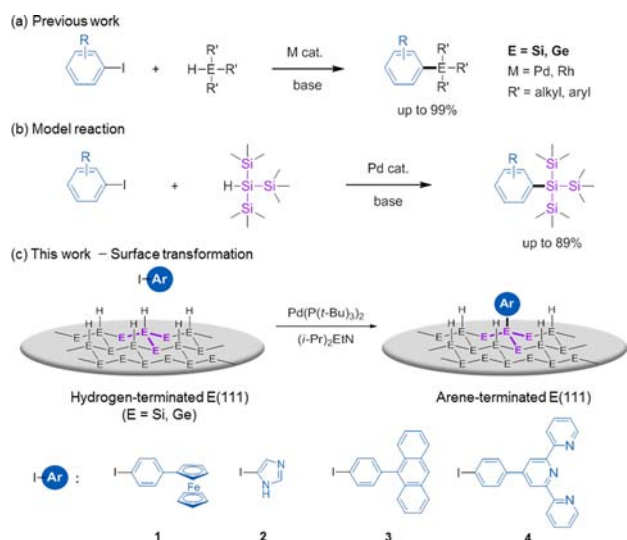


**Figure 1.** Synthetic scheme. (a) Transition metal-catalyzed arylation of hydrosilanes and hydrogermanes (previous work). (b) Pd-catalyzed arylation of tris(trimethylsilyl)silane (model reaction). (c) Pd-catalyzed surface reaction to immobilize aromatic group directly on hydrogen-terminated silicon(111) or germanium(111) surfaces (this work).

These compounds were identified using  $^1\text{H}$  and  $^{13}\text{C}$  NMR and EI-MS. Compounds **2** and **L** (tpy–C<sub>6</sub>H<sub>4</sub>–tpy) were purchased from TCI and Sigma-Aldrich, respectively.

#### Preparation of Hydrogen-Terminated Silicon(111) Surface.

The hydrogen-terminated Si(111) surface was prepared using a modification method based on our previous reports.<sup>21–24</sup> N-type silicon(111) wafers (for the immobilization of **1**, P doped, 0.001–0.013  $\Omega$  cm, E & M Co. Ltd. and for the immobilization of **3**, Sb doped, 0.01–0.03  $\Omega$  cm, SGI Japan Ltd.) and P-type silicon(111) wafers (for the immobilization of **2** and **4**, B doped,  $\leq 0.005$   $\Omega$  cm, E & M Co. Ltd.) were cut into squares (15  $\times$  15 mm). The wafers were cleaned ultrasonically in ultrapure water (Milli Q), ethanol, acetone, and ultrapure water (Milli Q) for 5 min to remove contaminations. The silicon wafers were then etched in a 1% HF aqueous solution at room temperature for 2 min and further etched in a 40% NH<sub>4</sub>F aqueous solution at 70  $^\circ\text{C}$  for 2 min to remove surface oxides and make the surfaces atomically flat. Finally, the wafers were taken out and rinsed thoroughly with ultrapure water, and then dried in a stream of argon gas. The samples for AFM measurements and for constructing the oligomer wires were hydrogen-terminated as follows.<sup>25</sup> The silicon wafers were immersed in piranha solution (conc. H<sub>2</sub>SO<sub>4</sub>:30% H<sub>2</sub>O<sub>2</sub> = 3:1) at 120  $^\circ\text{C}$  for 10 min and stored in ultrapure water (Milli Q). Just before use, the oxidized silicon wafers were immersed in 40% NH<sub>4</sub>F aqueous at room temperature for 10 min, and then rinsed thoroughly with ultrapure water and dried in a stream of argon gas.

**Preparation of Hydrogen-Terminated Germanium(111) Surface.** The hydrogen-terminated Ge(111) surface was prepared using a modification method based on the literature.<sup>26</sup> P-type germanium(111) wafers (B doped, 0.1–1.0  $\Omega$  cm, Tak materials Co. Ltd.) were cut into squares (15  $\times$  15 mm). The wafers were cleaned ultrasonically in ultrapure water (Milli Q), ethanol, acetone, and ultrapure water (Milli Q) for 5 min to remove contaminations. The germanium wafers were then immersed in a 47% HF aqueous solution at room temperature for 10 s, and then rinsed with ultrapure water. This procedure was repeated a total of five times before drying the samples in a stream of argon gas.

**Immobilization of Aryl Groups onto Hydrogen-Terminated Silicon(111) and Germanium(111) Surface.** The fresh hydrogen-terminated silicon(111) or germanium(111) wafers were added to a mixture of 1,4-dioxane, Pd(P(*t*-Bu)<sub>3</sub>)<sub>2</sub> (0.08 mM), (*i*-Pr)<sub>3</sub>EtN (0.3 M), and **1**, **2**, **3**, or **4** (8 mM) under a nitrogen atmosphere, and were

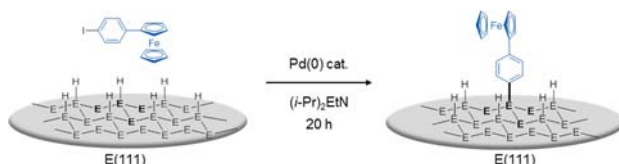
immersed at a constant temperature. After immersion, the samples were removed from the solution, and successively rinsed ultrasonically with 1,4-dioxane, ethanol, and ultrapure water (Milli Q) for 5 min. The modified wafers were dried in a stream of argon gas.

**Preparation of Fe(tpy)<sub>2</sub> Oligomer Wires.** The tpy-terminated wafers prepared in our method using a Pd catalyst were immersed in a 0.1 M ethanol solution of Fe(BF<sub>4</sub>)<sub>2</sub> at room temperature for 1 h, and subsequently in a 0.1 mM chloroform solution of 4',4''-(1,4-phenylene)bis(2,2':6',2''-terpyridine) (tpy–C<sub>6</sub>H<sub>4</sub>–tpy) for 23 h at room temperature to make bis(terpyridine) complexes. These two processes were repeated for the preparation of the Fe(tpy)<sub>2</sub> oligomer wires.

**Surface Characterization.** Electrochemical measurements were carried out using a modified silicon(111) or germanium(111) wafer as working electrode (electrode area: 0.264 cm<sup>2</sup>), a Pt wire counter electrode, and an Ag<sup>+</sup>/Ag (10 mM AgClO<sub>4</sub> in 0.1 M Bu<sub>4</sub>NClO<sub>4</sub>/CH<sub>3</sub>CN) reference electrode in a standard one-compartment cell in the dark. Cyclic voltammetry was performed using an ALS 750A or an ALS 650B electrochemical analyzer. Contact angle measurements were made by providing a 1  $\mu\text{L}$  drop of Milli-Q water from a microsyringe onto the surface of the sample and observing with an optical microscope. The image of the static water droplet was captured using a digital camera. Several measurements were taken on each side of the droplet for each sample, and the average water contact angle was calculated for the 20 individual samples. X-ray photoelectron spectroscopy (XPS) measurements were performed using a PHI5000 VersaProbe. Al K $\alpha$  (12 kV, 25 mA) was used as the X-ray source. The analyses were carried out at photoelectron angles (relative to the sample surface) of 5 $^\circ$ . Calibration of the spectra for ferrocene-containing film was achieved with C 1s spectrum at 285.0 eV (Figure S2, Supporting Information). That for 1H-imidazol-5-yl group immobilized silicon was achieved with Si 2p spectrum at 99.2 eV (Figure 3). The emission spectra and excitation spectra were recorded with a Hitachi FL-4500 spectrometer. AFM measurements were performed in high amplitude mode (tapping mode) using an Agilent Technologies 5500 scanning probe microscope, and a silicon cantilever PPP-NCH or PPP-NCL (Nano World).

## RESULTS AND DISCUSSION

For applying the homogeneous catalytic reaction to the surface modification, preliminary studies were carried out to optimize the immobilization of **1** on a hydrogen-terminated silicon surface. The hydrogen-terminated silicon surface was prepared by etching an oxidized Si surface in an HF and NH<sub>4</sub>F solution as described in our previous reports.<sup>21–24</sup> The surface coverage was estimated using cyclic voltammetry. As shown in Table 1, when the freshly prepared Si(111)–H surface was immersed in a mixture of 4-iodophenylferrocene (**1**), (*i*-Pr)<sub>3</sub>EtN, Pd(P(*t*-Bu)<sub>3</sub>)<sub>2</sub>, and 1,4-dioxane at 100  $^\circ\text{C}$  for 20 h, a modified surface with a Si–C bonded organic monolayer with good surface coverage was obtained (entry 5 in Table 1 and Figure 2a). The modified surface was rinsed successively with 1,4-dioxane, ethanol, and ultrapure water in an ultrasonic bath for a time of 5 min for each solvent. Longer rinsing did not decrease the surface coverage, indicating that the molecules were strongly attached to the surface and that there was no abrasion of the surface during the ultrasonic treatment. Other palladium catalysts, such as Pd(dba)<sub>2</sub> or Pd(PPh<sub>3</sub>)<sub>4</sub>, were less effective for this transformation (entries 3 and 4). As a control, the Si(111)–H surface was exposed to a mixture of **1** and base in the absence of a catalyst at 100  $^\circ\text{C}$  for 24 h. No immobilization of **1** was observed under these conditions (entry 6 in Table 1 and Figure 2a). The quantity of palladium catalyst used is important, and the formation of Pd nanoparticles (ca. 50 nm) on the surface was confirmed at intervals using AFM when the concentration of the palladium catalyst was higher (>ca. 0.8

Table 1. Optimization of Immobilization Process<sup>a</sup>


entry	E	Pd(0) catalyst	solvent	temperature (°C)	surface coverage $\Gamma$ ( $\times 10^{-10}$ mol/cm <sup>2</sup> ) <sup>b</sup>
1	Si	Pd(P( <i>t</i> -Bu) <sub>3</sub> ) <sub>2</sub>	THF	20	0.06
2	Si	Pd(P( <i>t</i> -Bu) <sub>3</sub> ) <sub>2</sub>	THF	50	0.24
3	Si	Pd(dba) <sub>2</sub>	THF	50	0.12
4	Si	Pd(PPh <sub>3</sub> ) <sub>4</sub>	THF	50	0.10
5	Si	Pd(P( <i>t</i> -Bu) <sub>3</sub> ) <sub>2</sub>	1,4-dioxane	100	2.6
6	Si	— <sup>c</sup>	1,4-dioxane	100	— <sup>c</sup>
7	Ge	Pd(P( <i>t</i> -Bu) <sub>3</sub> ) <sub>2</sub>	1,4-dioxane	100	0.69

<sup>a</sup>Reaction conditions: Si(111)–H or Ge(111)–H (15 × 15 mm) was immersed in a solution (7.5 mL) of catalyst (3.0 mg), (*i*-Pr)<sub>2</sub>EtN (0.38 mL), and **1** (0.06 mmol) for 20 h. <sup>b</sup>Average of several runs. <sup>c</sup>No aromatic compound was observed on the surface in the absence of Pd catalyst.

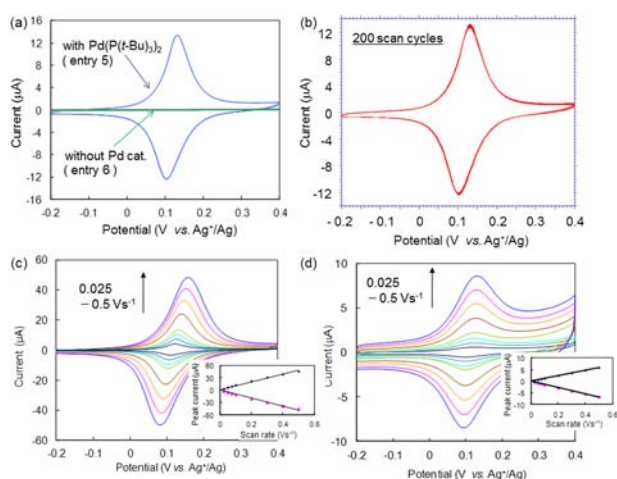


**Figure 2.** Electrochemical characterization of modified silicon or germanium surface. (a) CVs for entry 5 (Si(111)–1) and entry 6 in 1 M Bu<sub>4</sub>NClO<sub>4</sub>/CH<sub>3</sub>CN. (b) CVs for entry 5 (Si(111)–1) in 1 M Bu<sub>4</sub>NClO<sub>4</sub>/CH<sub>3</sub>CN with 200 scan cycles. (c) Characterization of Si(111)–1. (d) Characterization of Ge(111)–1. Cyclic voltammograms for (c) and (d) were carried out in 1 M Bu<sub>4</sub>NClO<sub>4</sub>/CH<sub>3</sub>CN. The scan rates were from 0.025 to 0.5 V s<sup>-1</sup>. (Inset) Plots of anodic and cathodic peak currents versus the scan rates.

mM) as shown in Figure S1, Supporting Information.<sup>27</sup> Although it was difficult to set palladium on surface to zero completely, XPS clearly showed that the amount of palladium on surface sharply decreased when palladium concentration was changed from 0.8 to 0.08 mM. The quantity of ferrocenyl (Fe<sup>2+</sup>) group was close to the same under both reaction conditions (Figure S2, Supporting Information). Under the same reaction conditions with entry 5, Ge(111)–H was also reacted with **1**, and a ferrocene-modified Ge surface was obtained (entry 7).<sup>26</sup> Because a Ge–Ge bond is longer than a Si–Si bond, the influence of a horizontal molecule becomes small when a self-assembled monolayer (SAM) is formed on the surface.

Cyclic voltammograms for monolayer films of ferrocene on N-type Si(111) and P-type Ge(111) in Bu<sub>4</sub>NClO<sub>4</sub>/CH<sub>3</sub>CN are shown in Figure 2. The redox peaks did not change at all, even when the potential sweep was repeated 200 times (Figure 2b). This showed that the modified surface prepared using this method had excellent durability, which resulted from the combination of the 4-ferrocenylphenyl groups with the silicon substrate via covalent Si–C bonds. A pair of anodic and cathodic waves was observed, with peak potentials located at approximately 0.1 V versus Ag<sup>+</sup>/Ag. The anodic and cathodic peak currents exhibited a linear dependence on the scan rate, indicating a surface confined redox process. By integrating the cathodic waves in the voltammograms, the surface coverage  $\Gamma$  was estimated to be  $2.6 \times 10^{-10}$  mol/cm<sup>2</sup> (Figure 2c). The monolayer coverage was estimated to be ca. 58%; this value was related to the unit cell size of Si(111) (12.77 Å<sup>2</sup>)<sup>28</sup> as compared to the diameter of the 4-ferrocenylphenyl group (38.0 Å<sup>2</sup>), and the maximum coverage of 4-ferrocenylphenyl groups on a silicon surface can be estimated to be  $4.5 \times 10^{-10}$  mol/cm<sup>2</sup>. The coverage of 4-ferrocenylphenyl groups on the germanium surface was similarly estimated to be ca. 15% (Figure 2d).

Water contact angle measurement and AFM were employed to investigate the properties of the modified silicon substrate. The silicon surfaces modified with 4-ferrocenylphenyl monolayer were more hydrophilic as shown by smaller contact angles obtained with H<sub>2</sub>O (45 ± 2°), as compared to those measured on hydrogen-terminated silicon (82 ± 5°) (Figure S3, Supporting Information).<sup>29</sup> The water contact angles measured in the present study were approximately consistent with other ferrocene-terminated SAMs.<sup>30,31</sup> The surface homogeneity of the modified silicon surface was confirmed in the AFM images (Figure S4, Supporting Information). The modified surface had terraces with the same width and atomic-thick steps similar to the hydrogen-terminated Si(111) surface. These results demonstrated that the prepared surfaces had uniform monolayer films.

The modified surface was also characterized using XPS, because useful information on the nature of the grafted layer was obtained (Figures S2 and S5, Supporting Information). A very weak Si 2p signal for silicon oxide (ca. 103 eV) was measured, due to the extended handling. Peaks for Fe 2p photoelectrons were observed at binding energies of 708.1 and 720.3 eV for the modified surface, indicating that the organic monolayer formed successfully on the silicon surface. These values agree well with those previously reported in the literature.<sup>31</sup> Peaks for C–Si (at approximately 284–285 eV) and C–C species are overlapped in the C 1s spectra and were not resolved under these measurement conditions.

To overcome these problems with the XPS measurements, 1*H*-imidazol-5-yl groups were immobilized on a hydrogen-terminated silicon surface (Figure 3a). The XPS spectra for the chemical species resulting from the treatment of 5-iodo-1*H*-imidazole (**2**) with H–Si(111) are shown in Figure 3. Figure 3b shows high-resolution C 1s spectra for the modified surface. Three peaks were observed; the peak at 284.7 eV represented the C 1s binding energy of hydrocarbon, and the other two peaks, located at 284.0 and 286.0 eV, in the shoulder of the main peak were assigned to Si–C and C–N species, respectively.<sup>32</sup> Figure 3c shows high-resolution Si 2p spectra for the modified surface. The spectra were divided into three components. The peak centers located at 99.2, 99.7, and 100.1 eV represented two elemental Si and Si–C, respectively. These results suggested that the aromatic groups were attached on the



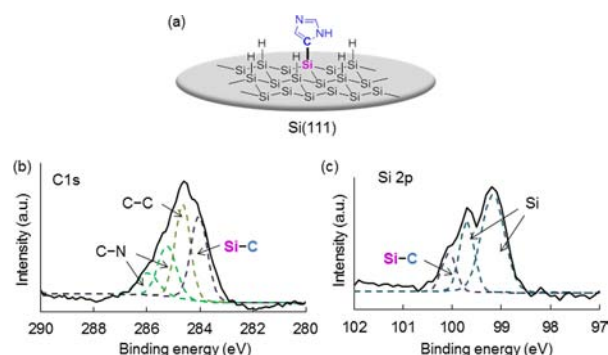


**Figure 3.** High-resolution XPS of Si(111) substrates after grafting of 1H-imidazol-5-yl group. The detector is  $5^\circ$  from the surface plane. (a) Structure of Si(111)-2. (b) C 1s region. (c) Si 2p region.

silicon surface through Si-C covalent bonds, and that any possible physisorption or alternative grafting onto the surface could be ruled out.

To give a further surface modification, the hydrogen-terminated Si(111) surface was treated with 9-(4-iodophenyl)anthracene (Ant-C<sub>6</sub>H<sub>4</sub>-I, **3**) in the presence of Pd catalyst at 100 °C for 20 h, using the method mentioned above (Figure S6, Supporting Information). Contact angle measurements confirmed the presence of terminal anthryl groups on the modified surface. The water contact angle obtained for the modified surface ( $73 \pm 3^\circ$ ) agreed well with previously reported values for anthracene-terminated SAMs.<sup>33</sup> Anthracene derivatives have been recognized as attractive materials because of their photochemical and electrochemical properties, as well as their potential as a medium for photoconductive and electroluminescent materials.<sup>34–36</sup> The fluorescence at approximately 420 nm, which derived from the Ant-C<sub>6</sub>H<sub>4</sub> moiety, appeared with the excitation at 254 nm (Figure 4). This

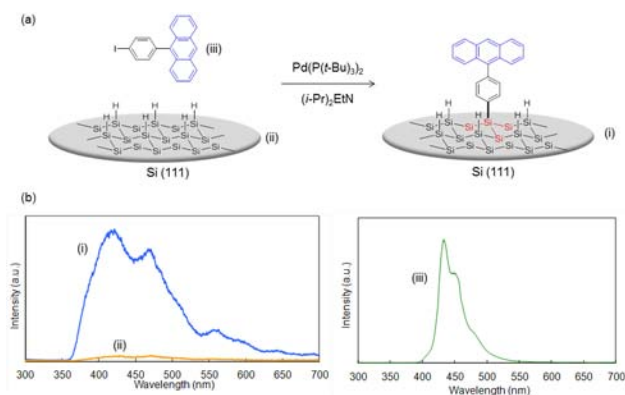


**Figure 4.** Preparation and characterization of Si(111)-3. (a) Immobilization of 9-(4-iodophenyl)anthracene (**3**) on Si(111). Si(111)-H was immersed in a 1,4-dioxane solution (7.5 mL) of Pd(P(*t*-Bu)<sub>3</sub>)<sub>2</sub> (3.0 mg), (*i*-Pr)<sub>2</sub>EtN (0.38 mL), and **3** (0.06 mmol) at 100 °C for 20 h. (b) Comparison of fluorescence spectra (254 nm excitation): (i) Si(111)-3, (ii) Si(111)-H, (iii) Ant-C<sub>6</sub>H<sub>4</sub>-I (**3**) in the solid state.

difference suggested that anthrylphenyl group was attached on the Si(111) surface as compared to the fluorescence of Ant-C<sub>6</sub>H<sub>4</sub>-I (**3**). The spectrum of Si(111)-3 displayed broader than that in the solid state (Figure 4b) or in solution (Figure S7, Supporting Information) due to a ground state  $\pi$ - $\pi$  stacking interaction in addition to excimer formation. Because

Tada and Ara reported that fluorescein isothiocyanate (FITC) was immobilized on silicon via three steps,<sup>37,38</sup> these observations demonstrated the possibility of potential applications in light emitting devices.

Finally, to further demonstrate the scope of this approach, we attempted to construct redox-active metal complex oligomer wires on a hydrogen-terminated Si(111) surface using subsequent complexation as described in previous reports from our laboratory.<sup>39–45</sup> The preparation of the oligomer wires was carried out as follows (Figure 5a). Because the coordination of Fe<sup>2+</sup> with tpy-C<sub>6</sub>H<sub>4</sub>-tpy was blocked when there was a high density of tpy-C<sub>6</sub>H<sub>4</sub> groups on the silicon surface, the hydrogen-terminated Si(111) surface was initially treated with 4'-(4-iodophenyl)-2,2':6',2''-terpyridine (tpy-C<sub>6</sub>H<sub>4</sub>-I, **4**) in the presence of Pd catalyst at 100 °C for 3 h as tpy-C<sub>6</sub>H<sub>4</sub> group can be sparsely fixed on the surface. The tpy-covered substrate was then immersed in a 0.1 M ethanol solution of Fe(BF<sub>4</sub>)<sub>2</sub> at room temperature for 1 h, and subsequently immersed in a 0.1 mM chloroform solution of 4',4'''-(1,4-phenylene)bis(2,2':6',2''-terpyridine) (tpy-C<sub>6</sub>H<sub>4</sub>-tpy, **L**) for 23 h. The [Fe(tpy)<sub>2</sub>]<sup>2+</sup> oligomer wires were constructed by repeating these two processes (the coordination of the Fe ions and the ligand).

Cyclic voltammetry was performed for the [Fe(tpy)<sub>2</sub>]<sup>2+</sup> oligomer wire-modified Si surface (denoted here as Si(111)-4-(FeL)<sub>n</sub>) to confirm the stepwise formation of wires on the Si surface (Figure S8, Supporting Information). The CV plots shown in Figure 5 exhibited redox peaks corresponding to the [Fe(tpy)<sub>2</sub>]<sup>3+/2+</sup> couple in oligomer wires, at a potential of approximately 0.8 V versus Ag<sup>+</sup>/Ag. The current waves of the peaks increased as the number of immersion cycles (*n*) increased. The coverage estimated from the cathodic peaks was proportional to *n*, which suggested that the preparation of the oligomer wires was quantitative. The anodic and cathodic peak currents of Si(111)-4-(FeL)<sub>10</sub> exhibited a linear dependence on the scan rate (Figure S9, Supporting Information), confirming that the molecular wires were confined on the surface.

The [Fe(tpy)<sub>2</sub>]<sup>2+</sup> oligomer wire growth process was observed using AFM. Figure 6a shows representative AFM images of Si(111)-4, Si(111)-4-(FeL)<sub>2</sub>, Si(111)-4-(FeL)<sub>4</sub>, and Si(111)-4-(FeL)<sub>10</sub>. In these four images, a number of convex structures were observed, which appeared to correspond with the formation of the Fe(tpy)<sub>2</sub> oligomer wires. The heights of these structures were  $1.2 \pm 0.2$ ,  $4.3 \pm 0.2$ ,  $7.3 \pm 0.4$ , and  $17.0 \pm 0.5$  nm (Figure 6b); these values were consistent with the theoretical height of Si(111)-4-(FeL)<sub>n</sub> (ca. 1.6 nm  $\times$  *n*-layers (oligomer wire moiety) + 1.1 nm (surface anchoring moiety)). The lengths of molecular wires were estimated by MM2 predictions. These results also suggested that oligomer wires were grown vertically on the Si surface, and that tpy-C<sub>6</sub>H<sub>4</sub>-I was immobilized on the Si surface via the Pd-catalyzed reaction (Figure S10, Supporting Information).

Our proposed mechanistic explanation for the Si-H surface arylation process is described in Figure 7. Initially, the dissociation of a phosphine ligand formed the monoligating Pd complex **A**. The resultant Pd(P(*t*-Bu)<sub>3</sub>) would be capable of undergoing oxidative addition with H-Si on the surface, generating the  $\sigma$ -bond metathesis intermediate **B** with aryl iodide, and then forming Si-C(sp<sup>2</sup>) bonds with the reforming active Pd catalyst in the presence of base. We do not think that dangling bonds (silicon radical:  $\equiv\text{Si}\bullet$ ) participated in the Si-C

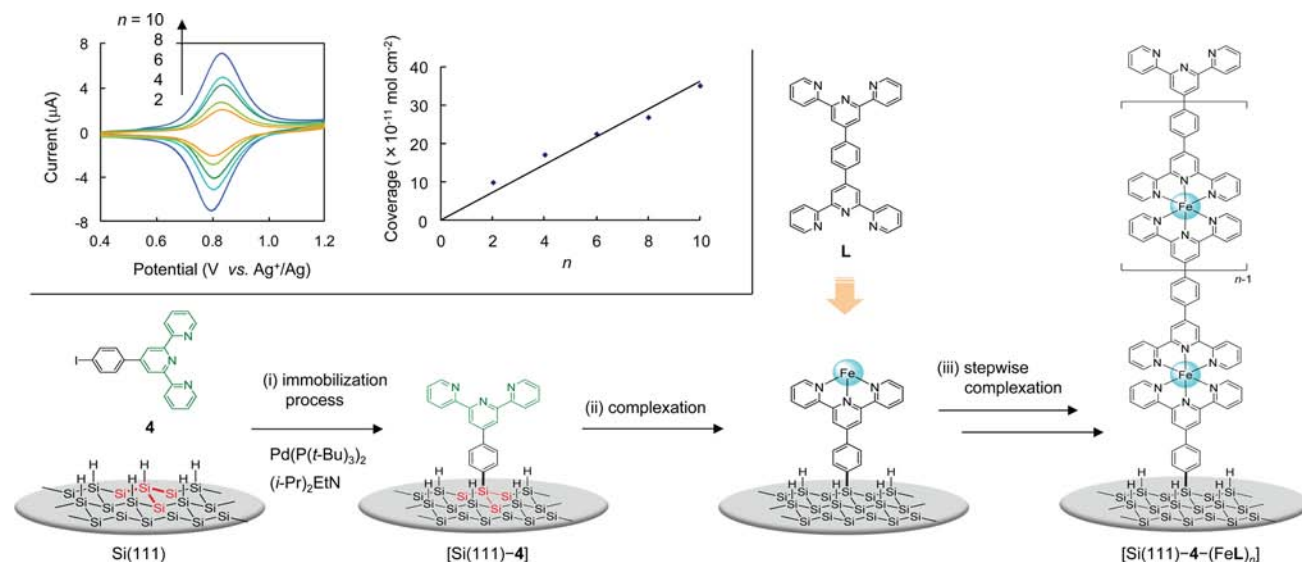


**Figure 5.** Preparation of Si(111)-4 and resulting oligomer wires. (i) Immobilization of 4'-(4-iodophenyl)-2,2':6',2''-terpyridine (**4**) on Si(111). Si(111)-H was immersed in a 1,4-dioxane solution (7.5 mL) of Pd(P(*t*-Bu)<sub>3</sub>)<sub>2</sub> (0.3 mg), (*i*-Pr)<sub>2</sub>EtN (0.38 mL), and **4** (0.06 mmol) at 100 °C for 3 h. (ii, iii) Preparation of Fe(tpy)<sub>2</sub> complex oligomer wires, Si(111)-4-(FeL)<sub>*n*</sub>. Inset: Cyclic voltammograms for Si(111)-4-(FeL)<sub>*n*</sub> (*n* = 1-4) taken at a scan rate of 0.1 V s<sup>-1</sup> in 1 M Bu<sub>4</sub>NClO<sub>4</sub>/CH<sub>2</sub>Cl<sub>2</sub> (left) and coverage of Si(111)-4-(FeL)<sub>*n*</sub> versus the number of coordination cycles (right).

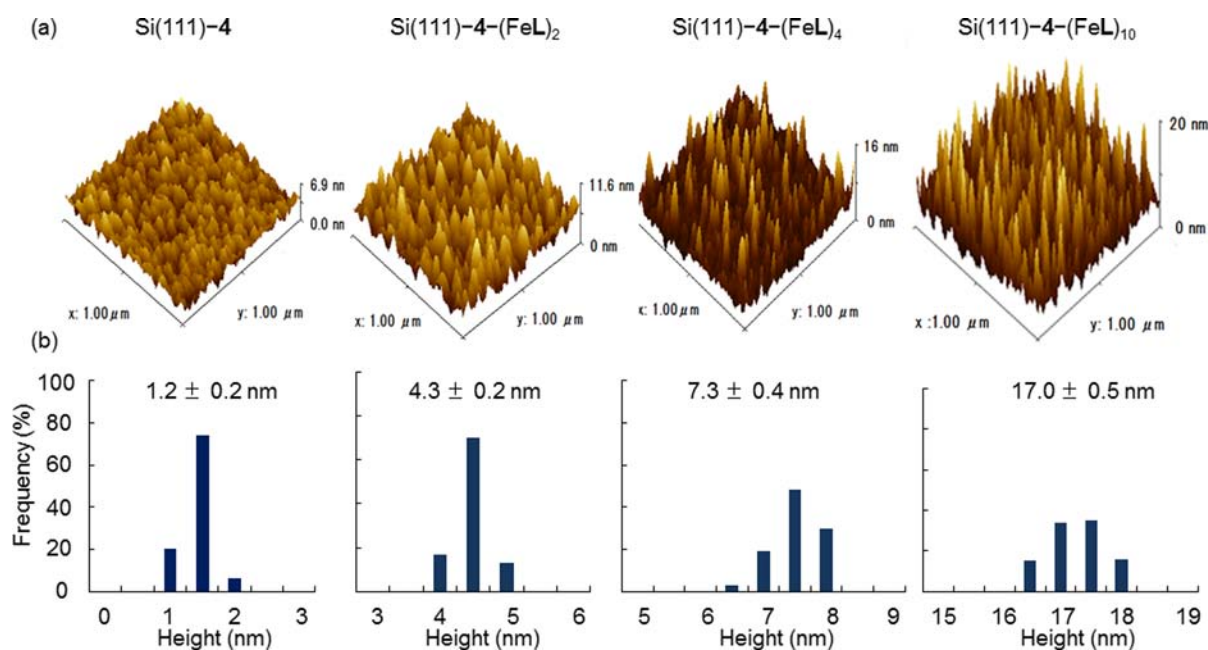


**Figure 6.** (a) Representative AFM images of Si(111)-4, Si(111)-4-(FeL)<sub>2</sub>, Si(111)-4-(FeL)<sub>4</sub>, and Si(111)-4-(FeL)<sub>10</sub>. (b) Histogram of height analyses of Si(111)-4, Si(111)-4-(FeL)<sub>2</sub>, Si(111)-4-(FeL)<sub>4</sub>, and Si(111)-4-(FeL)<sub>10</sub>.

bond formation, because tris(trimethylsilyl)silyl radical is an effective reducing species for organic halides.<sup>46</sup>

## CONCLUSIONS

This palladium-catalyzed grafting process was effective for 4-iodophenylferrocene (**1**), 5-iodo-1*H*-imidazole (**2**), 9-(4-iodophenyl)anthracene (**3**), and 4'-(4-iodophenyl)-2,2':6',2''-terpyridine (**4**), and gave the desired surface functionalization. The availability of a synthetic approach is key to the development of flexible surface synthesis strategies. Cyclic voltammetry, X-ray photoelectron spectroscopy, and AFM were used to characterize the surface and to estimate the surface

coverage. Although a few studies have investigated transition metal-catalyzed transformation onto hydrogen-terminated silicon surfaces,<sup>47-49</sup> problems result from substantial oxidation and metal deposition at the surface. The present results showed that covalently bonded aryl monolayers could be easily produced on Si(111) and Ge(111) surfaces via the chemical reaction of various aryl iodides with Si(111)-H or Ge(111)-H in the presence of a transition-metal catalyst. The attachment of these molecules was persistent and strong. The modified surfaces were chemically stable and could be stored for several weeks without measurable decomposition. This approach underpins the development of the stepwise solid-phase-like

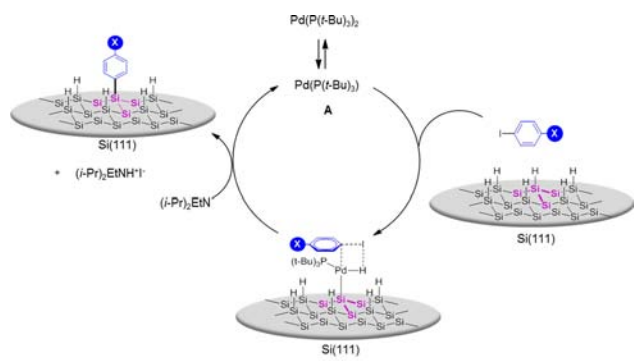


**Figure 7.** Proposed mechanistic pathway of Pd-catalyzed Si–H arylation on a hydrogen-terminated silicon(111) surface.

synthesis of complex molecular wires on surfaces. In future work, the immobilization of other functionalized aromatic monolayers on silicon and germanium surfaces will be investigated in our laboratory.

## ■ ASSOCIATED CONTENT

### 📄 Supporting Information

Compound characterization data and additional characterization data of the modified silicon(111) surface. This material is available free of charge via the Internet at <http://pubs.acs.org>.

## ■ AUTHOR INFORMATION

### Corresponding Author

yamanoi@chem.s.u-tokyo.ac.jp; nisihara@chem.s.u-tokyo.ac.jp

### Notes

The authors declare no competing financial interest.

## ■ ACKNOWLEDGMENTS

The present work was financially supported by Grant-in-Aids from the Ogasawara Foundation for the Promotion of Science & Engineering, Scientific Research on Innovative Areas “Coordination Programming” (area 2107, no. 21108002), and the Global COE Program for “Chemistry Innovation through the Cooperation of Science and Engineering” from the Ministry of Education, Culture, Sports, Science, and Technology, Japan. We thank the Research Hub Advanced Nano Characterization (School of Engineering, The University of Tokyo) for the X-ray photoelectron spectroscopy measurements and also thank ADEKA Corp. for their financial support throughout this work.

## ■ REFERENCES

- (1) Ciampi, S.; Harper, J. B.; Gooding, J. J. *Chem. Soc. Rev.* **2010**, *39*, 2158–2183.
- (2) Buriak, J. M. *Chem. Rev.* **2002**, *102*, 1271–1308.
- (3) Wayner, D. D. M.; Wolkow, R. A. J. *Chem. Soc., Perkin Trans. 2* **2002**, *23*–34.
- (4) Buriak, J. M. *Chem. Commun.* **1999**, 1051–1060.
- (5) de Villeneuve, C. H.; Pinson, J.; Bernard, M. C.; Allongue, P. J. *Phys. Chem. B* **1997**, *101*, 2415–2420.
- (6) Stewart, M. P.; Maya, F.; Kosynkin, D. V.; Dirk, S. M.; Stapleton, J. J.; McGuinness, C. L.; Allara, D. L.; Tour, J. M. *J. Am. Chem. Soc.* **2004**, *126*, 370–378.
- (7) Scott, A.; Janes, D. B. *J. Appl. Phys.* **2009**, *105*, 073512.
- (8) Pandey, D.; Zemlyanov, D. Y.; Bevan, K.; Reifengerger, R. G.; Dirk, S. M.; Howell, S. W.; Wheeler, D. R. *Langmuir* **2007**, *23*, 4700–4708.
- (9) Dirk, S. M.; Pylypenko, S.; Howell, S. W.; Fulghum, J. E.; Wheeler, D. R. *Langmuir* **2005**, *21*, 10899–10901.

- (10) Yamanoi, Y. *J. Org. Chem.* **2005**, *70*, 9607–9609.
- (11) Yamanoi, Y.; Nishihara, H. *Tetrahedron Lett.* **2006**, *47*, 7157–7161.
- (12) Yamanoi, Y.; Taira, T.; Sato, J.-i.; Nakamura, I.; Nishihara, H. *Org. Lett.* **2007**, *9*, 4543–4546.
- (13) Yamanoi, Y.; Nishihara, H. *J. Org. Chem.* **2008**, *73*, 6671–6678.
- (14) Yamanoi, Y.; Nishihara, H. *J. Synth. Org. Chem. Jpn.* **2009**, *67*, 778–786.
- (15) Yabusaki, Y.; Ohshima, N.; Kondo, H.; Kusamoto, T.; Yamanoi, Y.; Nishihara, H. *Chem.-Eur. J.* **2010**, *16*, 5581–5585.
- (16) Lesbani, A.; Kondo, H.; Yabusaki, Y.; Nakai, M.; Yamanoi, Y.; Nishihara, H. *Chem.-Eur. J.* **2010**, *16*, 13519–13527.
- (17) Kurihara, Y.; Nishikawa, M.; Yamanoi, Y.; Nishihara, H. *Chem. Commun.* **2012**, *48*, 11564–11566.
- (18) Lesbani, A.; Kondo, H.; Sato, J.-i.; Yamanoi, Y.; Nishihara, H. *Chem. Commun.* **2010**, *46*, 7784–7786.
- (19) Winters, M. U.; Dahlstedt, E.; Blades, H. E.; Wilson, C. J.; Frampton, M. J.; Anderson, H. L.; Albinsson, B. *J. Am. Chem. Soc.* **2007**, *129*, 4291–4297.
- (20) Alemán, E. A.; Shreiner, C. D.; Rajesh, C. S.; Smith, T.; Garrison, S. A.; Modarelli, D. A. *Dalton Trans.* **2009**, 6562–6577.
- (21) Yamanoi, Y.; Yonezawa, T.; Shirahata, N.; Nishihara, H. *Langmuir* **2004**, *20*, 1054–1056.
- (22) Yamanoi, Y.; Shirahata, N.; Yonezawa, T.; Terasaki, N.; Yamamoto, N.; Matsui, Y.; Nishio, K.; Masuda, H.; Ikuhara, Y.; Nishihara, H. *Chem.-Eur. J.* **2006**, *12*, 314–323.
- (23) Yonezawa, T.; Uchida, K.; Yamanoi, Y.; Horinouchi, S.; Terasaki, N.; Nishihara, H. *Phys. Chem. Chem. Phys.* **2008**, *10*, 6925–6927.
- (24) Uchida, K.; Yamanoi, Y.; Yonezawa, T.; Nishihara, H. *J. Am. Chem. Soc.* **2011**, *133*, 9239–9241.
- (25) Yamada, T.; Kawai, M.; Wawro, A.; Suto, S.; Kasuya, A. *J. Chem. Phys.* **2004**, *121*, 10660–10667.
- (26) Deegan, T.; Hughes, G. *Appl. Surf. Sci.* **1998**, *123/124*, 66–70.
- (27) Sugimura, H.; Hanji, T.; Takai, O.; Masuda, T.; Misawa, H. *Electrochim. Acta* **2001**, *47*, 103–107.
- (28) Sieval, A. B.; Linke, R.; Zuilhof, H.; Sudhölter, E. J. R. *Adv. Mater.* **2000**, *12*, 1457–1460.
- (29) Liu, Y.-J.; Navasero, N. M.; Yu, H.-Z. *Langmuir* **2004**, *20*, 4039–4050.
- (30) Tajimi, N.; Sano, H.; Murase, K.; Lee, K.-H.; Sugimura, H. *Langmuir* **2007**, *23*, 3193–3198.
- (31) Sondag-Huethorst, J. A. M.; Fokkink, L. G. J. *Langmuir* **1994**, *10*, 4380–4387.
- (32) Wagner, C. D.; Riggs, W. M.; Davis, L. E.; Moulder, J. F.; Muilenberg, G. E. *Handbook of X-Ray Photoelectron Spectroscopy*; Perkin-Elmer: Eden Prairie, MN, 1979; pp 38–41, 52–53, and 76–77.
- (33) Fox, M. A.; Wooten, M. D. *Langmuir* **1997**, *13*, 7099–7105.
- (34) Tyson, D. S.; Bignozzi, C. A.; Castellano, F. N. *J. Am. Chem. Soc.* **2002**, *124*, 4562–4563.
- (35) Vaes, A.; Van der Auweraer, M.; Bosmans, P.; De Schryver, F. C. *J. Phys. Chem. B* **1998**, *102*, 5451–5459.
- (36) Durfee, W. S.; Storck, W.; Willig, F.; von Frieling, M. *J. Am. Chem. Soc.* **1987**, *109*, 1297–1301.
- (37) Tada, H.; Ara, M.; Tanaka, S. *Mater. Res. Soc. Symp. Proc.* **2003**, *739*, 113–117.
- (38) Ara, M.; Tsuji, M.; Tada, H. *Surf. Sci.* **2007**, *601*, 5098–5102.
- (39) Maeda, H.; Sakamoto, R.; Nishimori, Y.; Sendo, J.; Toshimitsu, F.; Yamanoi, Y.; Nishihara, H. *Chem. Commun.* **2011**, *47*, 8644–8646.
- (40) Kurita, T.; Nishimori, Y.; Toshimitsu, F.; Muratsugu, S.; Kume, S.; Nishihara, H. *J. Am. Chem. Soc.* **2010**, *132*, 4524–4525.
- (41) Nishimori, Y.; Kanaizuka, K.; Kurita, T.; Nagatsu, T.; Segawa, Y.; Toshimitsu, F.; Muratsugu, S.; Utsuno, M.; Kume, S.; Murata, M.; Nishihara, H. *Chem.-Asian J.* **2009**, *4*, 1361–1367.
- (42) Nishimori, Y.; Kanaizuka, K.; Murata, M.; Nishihara, H. *Chem.-Asian J.* **2007**, *2*, 367–376.
- (43) Kanaizuka, K.; Murata, M.; Nishimori, Y.; Mori, I.; Nishio, K.; Masuda, H.; Nishihara, H. *Chem. Lett.* **2005**, *34*, 534–535.

- (44) Miyachi, M.; Ohta, M.; Nakai, M.; Kubota, Y.; Yamanoi, Y.; Yonezawa, T.; Nishihara, H. *Chem. Lett.* **2008**, *37*, 404–405.
- (45) Yamanoi, Y.; Nishihara, H. *Chem. Commun.* **2007**, 3983–3989.
- (46) Chatgililoglu, C. *Organosilanes in Radical Chemistry*; Wiley: Chichester, 2004; pp 53–69.
- (47) Mizuno, H.; Buriak, J. M. *J. Am. Chem. Soc.* **2008**, *130*, 17656–17657.
- (48) Zazzera, L. A.; Evans, J. F.; Deruelle, M.; Tirrell, M.; Kessel, C. R.; Mckeown, P. J. *Electrochem. Soc.* **1997**, *144*, 2184–2189.
- (49) Holland, J. M.; Stewart, M. P.; Allen, M. J.; Buriak, J. M. *J. Solid State Chem.* **1999**, *147*, 251–258.